nature climate change

Article

https://doi.org/10.1038/s41558-022-01545-9

Global warming overshoots increase risks of climate tipping cascades in a network model

Received: 4 March 2022

Accepted: 3 November 2022

Published online: 22 December 2022

Check for updates

Nico Wunderling[1,2,3] ✉, Ricarda Winkelmann[1,4], Johan Rockström[1,2], Sina Loriani[1], David I. Armstrong McKay[2,5,6], Paul D. L. Ritchie[5], Boris Sakschewski[1] & Jonathan F. Donges[1,2,3] ✉

Current policies and actions make it very likely, at least temporarily, to overshoot the Paris climate targets of 1.5–<2.0 °C above pre-industrial levels. If this global warming range is exceeded, potential tipping elements such as the Greenland Ice Sheet and Amazon rainforest may be at increasing risk of crossing critical thresholds. This raises the question of how much this risk is amplified by increasing overshoot magnitude and duration. Here we investigate the danger for tipping under a range of temperature overshoot scenarios using a stylized network model of four interacting climate tipping elements. Our model analysis reveals that temporary overshoots can increase tipping risks by up to 72% compared with non-overshoot scenarios, even when the long-term equilibrium temperature stabilizes within the Paris range. Our results suggest that avoiding high-end climate risks is possible only for low-temperature overshoots and if long-term temperatures stabilize at or below today's levels of global warming.

It has long been proposed that important continental-scale subsystems of Earth's climate system possess nonlinear behaviour[1,2]. The defining property of these tipping elements is their self-perpetuating feedbacks once a critical threshold is transgressed[3] such as the melt–elevation feedback for the Greenland Ice Sheet[4] and the moisture recycling feedback for the Amazon rainforest[5]. The global mean surface temperature has been identified as the driving parameter for the state of the climate tipping elements[1,6,7], which include, among others, systems such as the large ice sheets on Greenland and Antarctica, the Atlantic meridional overturning circulation (AMOC) and the Amazon rainforest[8–11].

Besides further amplifying anthropogenic global warming[3], the disintegration of such climate tipping elements individually would have large consequences for the biosphere and human societies, including large-scale sea-level rise or biome collapses. Since the first mapping of climate tipping elements in 2008[1], the scientific focus has increased, with a 2019 warning that 9 of the 15 known climate tipping elements are showing signs of instability[12], followed by a listing of all known climate tipping elements with expert judgements of tipping-point confidence levels in Working Group I's contribution to the Sixth Assessment Report of the IPCC[13]. While the uncertainty for crossing tipping points is still stated as medium to high, the IPCC concludes that crossing them triggering potentially abrupt changes cannot be excluded from projected future global warming trajectories[13]. As this science has advanced over the past two decades, potential temperature thresholds have been corrected downwards several times[12]. The most recent scientific assessment places the critical threshold temperatures of triggering tipping points at 1–5 °C, with moderate risks already at 1.5–2.0 °C for several systems, such as the Greenland and West Antarctic ice sheets[6]. In this sense, tipping-elements research provides even further scientific support to hold global mean surface temperatures within the Paris range of well below 2 °C while at the same time emphasizing that tipping-point risks cannot be ruled out even at this lower temperature range[6,7]. There is thus a triple dilemma emerging here. First, insufficient policies and actions mean that the world is following a trajectory well beyond 2 °C by the end of this century[14]. Second, essentially all IPCC scenarios that hold

[1]FutureLab Earth Resilience in the Anthropocene, Potsdam Institute for Climate Impact Research (PIK), Member of the Leibniz Association, Potsdam, Germany. [2]Stockholm Resilience Centre, Stockholm University, Stockholm, Sweden. [3]High Meadows Environmental Institute, Princeton University, Princeton, NJ, USA. [4]Institute of Physics and Astronomy, University of Potsdam, Potsdam, Germany. [5]Faculty of Environment, Science and Economy, University of Exeter, Exeter, UK. [6]Georesilience Analytics, Leatherhead, UK. ✉e-mail: nico.wunderling@pik-potsdam.de; jonathan.donges@pik-potsdam.de

the 1.5 °C line include a period of several decades of temperature overshoot[13,15,16]. And third, although given the large uncertainties among the different assessments[13,17], research cannot exclude the crossing of tipping-point thresholds already at low temperature rise[6]. Therefore, more knowledge is urgently needed on which overshoots still allow for low tipping risks[18–20].

Hence, it is essential to assess temperature overshoots and long-term temperature stabilization levels that can lead to irreversible changes in the climate system. While the impacts of overshoots have been investigated from a mathematical point of view and for individual climate tipping elements[18,21,22], they interact across scales in space and time, creating risks for additional feedback dynamics[12,23–25]. Interactions may increase tipping risks by triggering cascades when a transition of one element triggers transitions of connected tipping elements[26]. Therefore, in this work, we combine interactions between climate tipping elements and temperature overshoots in a stylized network model. We designed (stylized) our model to be able to perform tipping-risk assessments, but it should not be used to make predictions. We systematically assess the risk for tipping and identify a high climate-risk zone, considering remaining uncertainties in the properties of the tipping elements and different global warming overshoot scenarios if Paris temperature targets are not met without overshoots.

Modelling approach

Following Wunderling et al.[26], we use a stylized network model of four coupled ordinary differential equations designed for the analysis of risk assessments, which couples four climate tipping elements (Methods): the Greenland Ice Sheet, West Antarctic Ice Sheet, AMOC and Amazon rainforest (Fig. 1c). We assume that each of the four elements is a climate tipping element, exhibiting a critical transition at its respective critical temperature threshold (Methods and equation (1))[6,27]. Although there is considerable uncertainty in complex climate models whether and at which global warming level the exact tipping point is located[13,17], evidence from models of varying complexity, data-based approaches and palaeoclimate observations are consistent with considerable risks for nonlinearities among them[6] (Supplementary Section 1). However, there are negative feedbacks, such as the Planck feedback, CO_2 fertilization, ocean solubility of CO_2 and ocean heat uptake, that stabilize the climate system[13,28,29]. Those negative feedbacks, generally well represented already in climate models (compared with the tipping elements explored in this paper), might modify the tipping properties of some tipping elements. For example, the positive ice–albedo feedback despite competition with the negative Planck feedback has been shown to induce two stable large-scale Earth system states, a snowball Earth and a warm state[30,31]. On the smaller scale of climate tipping elements, the Planck feedback would be large if the global mean temperature increase from disintegrating climate tipping elements is large because the Planck feedback operates on the global mean temperature. At least for the large ice sheets on Greenland and West Antarctica, however, this effect may be limited since their complete disappearance would lead to a global warming of less than 0.2 °C in total[32]. By contrast, although the Amazon rainforest is stated to lose resilience[33], the formation of spatial patterns[34,35] and climate change may not affect all parts of the Amazon rainforest equally[36] and could prevent a single system-wide tipping event.

Nevertheless, we argue that sufficient evidence exists for climate tipping points to justify a risk analysis approach based on the precautionary principle. It is important to quantify tipping risks because the likelihood of tipping points existing is nonzero, and if they exist, they present high climate risks for the biosphere and human societies[6,12]. This has been re-emphasized in a recent study remarking that current risk assessments of high-end climate change scenarios (including tipping elements) are dangerously underexplored[37,38]. Simplified representations of more complex phenomena is a useful modelling approach in this context for capturing broad-scale patterns and risks.

Since the four tipping elements are not individual subsystems, we conceptualize the interactions as linear couplings in our model (equation (1)). Each of these interactions has a driving physical mechanism behind it (Fig. 1c), which was coarsely quantified by a formalized expert elicitation[25]. While these interaction estimates were coarse, newer literature confirms and substantiates them[26,39–41], enabling us to assess cascading tipping risks at a certain level of global warming. For further details on the exact nature of the interactions, see Fig. 1c and ref. 26.

Overall, our network model is able to capture the main dynamics of these four interacting tipping elements and is therefore able to propagate important uncertainties in the input parameters. It is designed to assess the risk for critical transitions but can, as such, not be used for predictions or to assess whether tipping points exist, but their existence is an a priori assumption in this work. Important model uncertainties include critical temperature thresholds, interaction strengths and interaction network structures, as well as typical transition timescales of individual tipping elements (Methods and Supplementary Table 1). In this Article, the transition timescale is the time that is needed for a transition from the baseline to the transitioned regime for an individual (non-interacting) climate tipping element as compiled in recent literature (compare Fig. 1)[6]. The low computational complexity of our approach allows to sample the parameter space by means of a very large-scale Monte Carlo ensemble, including approximately 4.455 million individual ensemble members in total. For the construction of the ensemble, but also for the boundary values of the parameters uncertainties (based on the latest literature review[6]), see Methods. Last, there is uncertainty not only in model parameters but also in the assumed (fold-bifurcation) structure of the tipping elements themselves due to negative feedbacks, at different strengths, modifying the bifurcation structure. This uncertainty can be taken into account by altering the prefactors of the cubic and linear terms of equation (1). Therefore, it would be possible to probe scenarios where some of the tipping elements are weak (or not) nonlinear systems. However, since exact values for these prefactors cannot be straightforwardly derived from existing data, such a sensitivity assessment is beyond the scope of this work. More important, our present study focuses on the high-end risk case where all considered climate subsystems possess tipping points.

In our numerical experiments, the four-tipping-element network is exposed to different global warming overshoot scenarios characterized by peak temperature, overshoot duration and the final convergence temperature reached in long-term equilibrium (Fig. 1a). All these important properties of the overshoot trajectory determine the potential of a tipping event. The stylized temperature overshoot trajectories applied to the four interacting climate tipping elements were designed primarily to capture typical temperature profiles generated by Earth system model simulations for low- to medium-emission scenarios[42]. Moreover, the formulation of the trajectories allows for flexibility in how society manages the transition from current warming to the convergence temperature, which can therefore lead to overshoot trajectories[18]. To this end, our ensemble spans all combinations of (1) peak temperatures $T_{\mathrm{Peak}} = 2.0, 2.5, \ldots, 6.0$ °C (maximally reached temperature), (2) convergence temperatures $T_{\mathrm{Conv}} = 0.0, 0.5, \ldots, 2.0$ °C (final stabilization temperature) and (3) convergence times $t_{\mathrm{Conv}} = 100, 200, \ldots, 1{,}000$ yr (time to reach T_{Conv}), allowing us to quantify the respective risk and timescale for tipping events. Note that the limit case of $T_{\mathrm{Peak}} = T_{\mathrm{Conv}} = 2.0$ °C is simulated as constant temperature. In this Article, we will focus on peak temperatures up to 4.0 °C, where 4.0 °C represents an upper temperature limit we investigate, based on policies and targets following COP26 and the Climate Action Tracker[14]. High-end warming scenarios with peak temperatures of 4.5–6.0 °C are added in the Extended Data figures, which allow computing a comprehensive risk analysis. Figure 1a presents an exemplary timeline of an overshoot trajectory that peaks at 2.5 °C warming and converges to a 2.0 °C convergence temperature after 400 years. The impact on the four studied interacting tipping elements is shown in Fig. 1b (for

https://doi.org/10.1038/s41558-022-01545-9

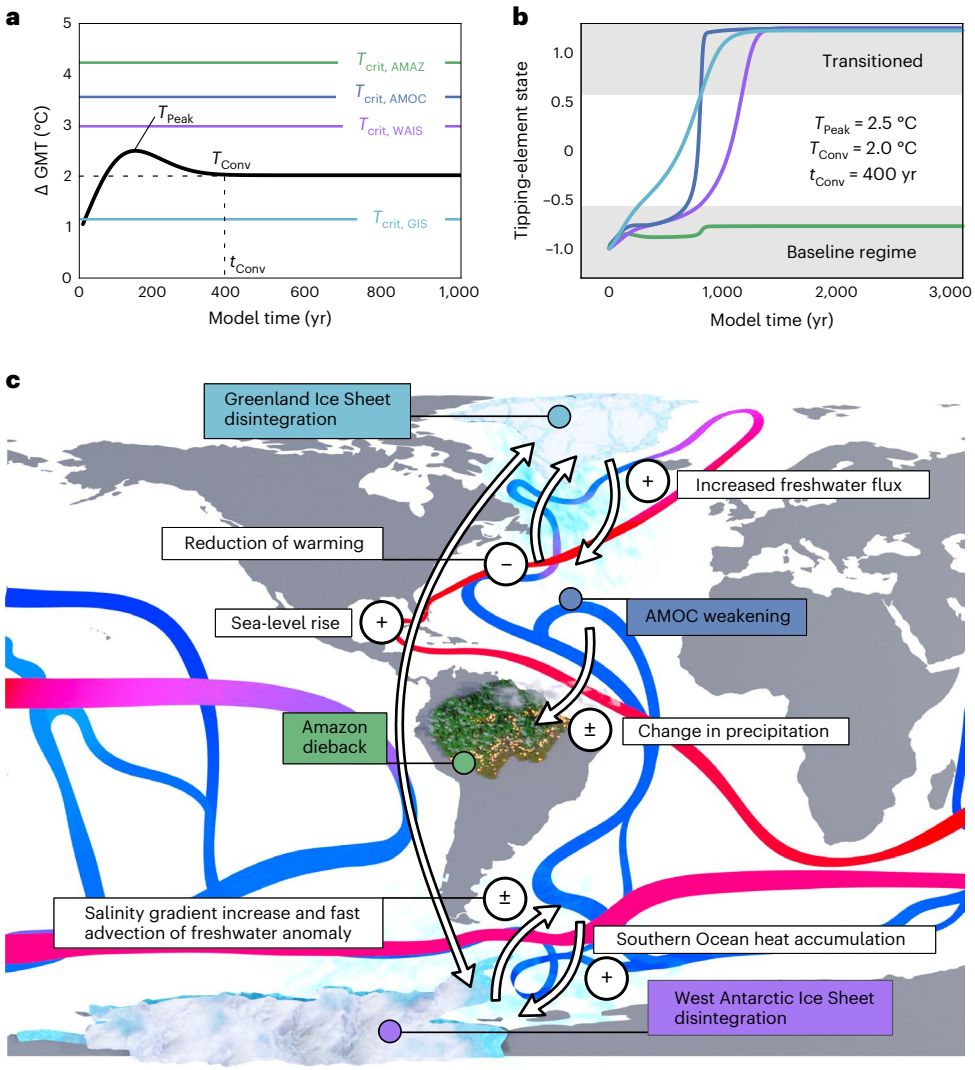

Fig. 1 | Interacting climate tipping elements. a, Exemplary global warming overshoot scenario with a peak temperature of T_{Peak} = 2.5 °C, a convergence temperature of T_{Conv} = 2.0 °C above pre-industrial and a time to convergence to 2.0 °C of t_{Conv} = 400 yr. This scenario is applied to a set of four interacting climate tipping elements with an exemplary draw of critical thresholds from their full uncertainty ranges (Supplementary Table 1). **b**, The effect of the overshoot trajectory shown in **a**: the Greenland Ice Sheet, the West Antarctic Ice Sheet and the AMOC tip. The grey shaded areas depict the two possible states, either not tipped (baseline regime) or tipped (transitioned) state. **c**, Map of the four interacting climate tipping elements. Each arrow represents a physical interaction mechanism between a pair of tipping elements, which can be destabilizing (denoted as +), stabilizing (denoted as −) or unclear (denoted as ±). AMAZ, Amazon rainforest; GIS, Greenland Ice Sheet; WAIS, West Antarctic Ice Sheet. The underlying map in **c** has been created with cartopy[61].

further examples, see Extended Data Fig. 1). In the remainder of this work, the impact of a certain relevant parameter combination (T_{Peak}, T_{Conv}, t_{Conv}) on the risk of an element tipping is given by the fraction of all simulation runs that result in the transitioned regime, averaged over all other parameters and uncertainties. We define the tipping of an element as the tipping process being completed, that is, when the tipping element reaches the transitioned regime (compare Fig. 1b). We first evaluate the tipping risk with respect to the overshoot peak temperature, convergence temperature and convergence time and identify risk maps for a high climate-risk zone. After that, we determine the mechanisms and reasons for tipping events.

The effects of overshoot peak temperature

Focusing on the role of overshoot peak temperature, we find that the risk for the emergence of at least one tipping event increases with rising peak temperature. Averaged over all ensemble members, around one-third (36.5 ± 5.0%) of all simulations show a tipping event or cascade at a peak temperature of 2.0 °C, while it is close to three-quarters (74.3 ± 1.4%) of all simulations at 4.0 °C peak temperature (Fig. 2a). However, the dependence on the peak temperature is unevenly distributed among the four climate tipping elements (Fig. 2b). The tipping risk for tipping elements with high inertia (slow-tipping elements: Greenland and West Antarctic ice sheets) remains relatively constant over an increasing peak temperature because their reaction time (500–13,000 yr) is slow against the duration of the overshoot trajectory (t_{Conv} = 100–1, 000 years). Therefore, the tipping risk for the Greenland Ice Sheet remains relatively constant between 14.0 ± 5.7% (T_{Peak} = 2.0 °C) and 16.0 ± 3.5% (T_{Peak} = 4.0 °C; Fig. 2b). By contrast, for tipping elements with low inertia (fast-tipping elements: AMOC and Amazon rainforest), there is a strong tipping-risk increase, comparing 24.7 ± 3.7% (T_{Peak} = 2.0 °C) with 50.8 ± 4.4% (T_{Peak} = 4.0 °C; Fig. 2b) for the AMOC. However, the tipping risk for the slow-tipping elements increases for increasing convergence times (Extended Data Fig. 3), whereas the tipping risk for the fast-tipping elements increases only slightly for increasing convergence times above 200 yr. This subsequent increase can be attributed largely to cascading effects, where

https://doi.org/10.1038/s41558-022-01545-9

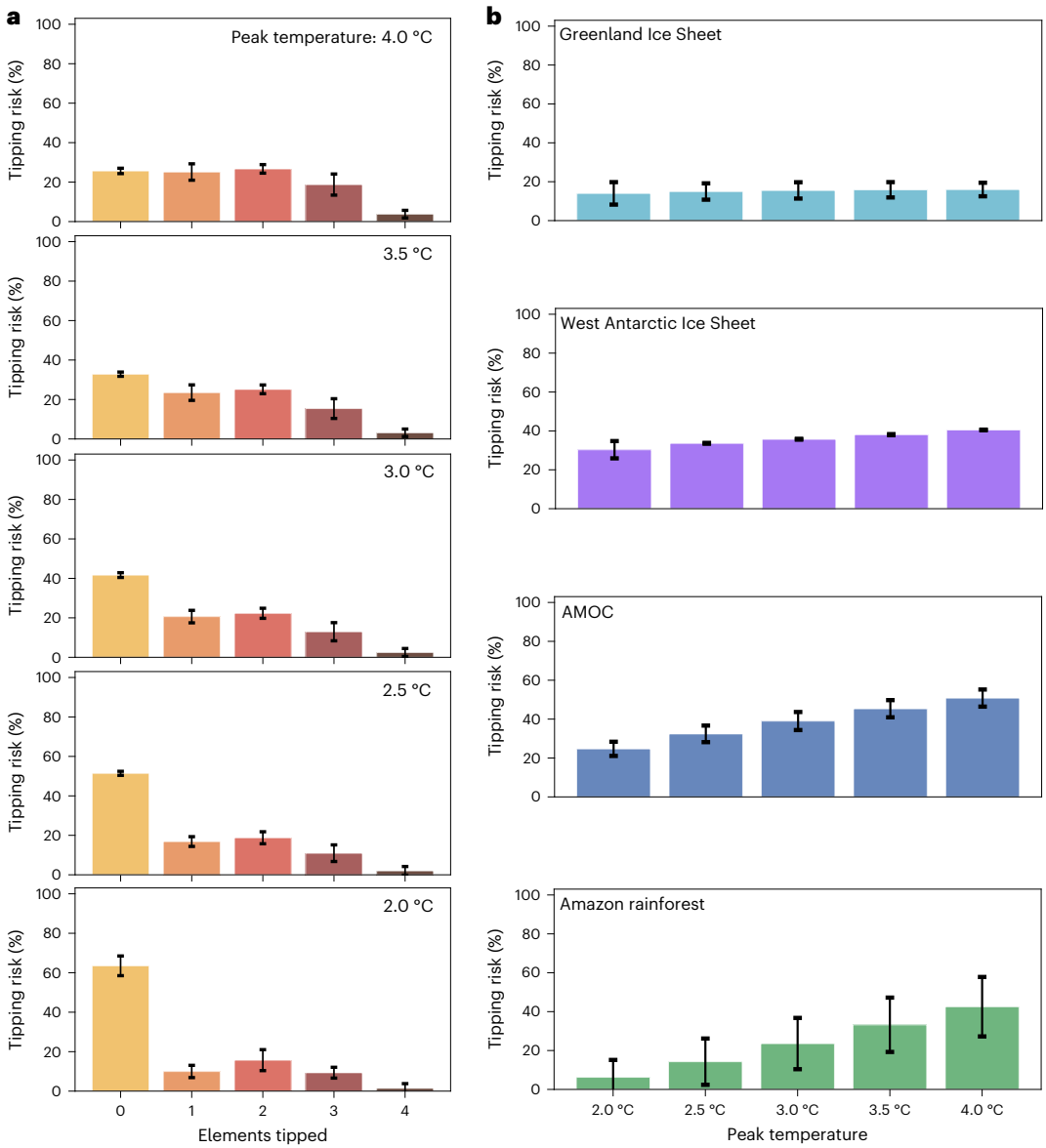

Fig. 2 | Effect of overshoot peak temperature. a, Number of tipped elements crossing tipping points due to additional forcing at overshoot peak temperatures of 2.0–4.0 °C above pre-industrial levels. Colours from yellow to dark red denote the number of tipped elements (0, 1, 2, 3, or 4). **b**, Risk for the individual climate tipping elements of transitioning into the undesired state crossing tipping points at overshoot peak temperatures of 2.0–4.0 °C. The bar colours denote the respective colour of the individual climate tipping element as in Fig. 1a,b. We depict the average of the equilibrium run (long-term tipping after 50,000 simulation years) over the entire ensemble as the bar height, and the error bars show the standard deviation. High-end overshoot peak temperatures up to 6.0 °C above pre-industrial levels and transition times (after 100 yr, after 1,000 yr and in equilibrium) are shown in Extended Data Fig. 2.

typically the Greenland Ice Sheet tipping has initiated tipping on the faster elements. Figure 2 shows the equilibrium results after 50,000 simulation years, which demonstrates the long-term commitment due to transgressed tipping thresholds. While this provides an important insight into potential locked-in change, some tipping risks are already realized after 100–1,000 yr. On these shorter timescales, especially the AMOC and the Amazon rainforest show a strong dependence on the peak temperature (Extended Data Fig. 2).

Risk maps for identifying a high climate-risk zone

For final convergence temperatures comparable with today's levels of warming (approximately T_{Conv} = 1.0 °C), we find that the expected number of tipped elements is at least $< \# >_{tipped,min} = 0.29$ (Fig. 3a). This minimal number of tipped elements is evaluated for the most optimistic case of this study (lowest-left parameter combination in Fig. 3), where the peak temperature reaches 2.0 °C above pre-industrial and the convergence time is 100 yr. The tipping risk that at least one tipping element transitions to its alternative state (related to $< \# >_{tipped,min} = 0.29$) is 15% (Fig. 3d). Stabilizing global warming at the lower (upper) limit of the Paris range at 1.5 °C (2.0 °C) above pre-industrial levels increases the number of minimally tipped elements (to 1.19 and 1.89; Fig. 3b,c).

We define a high climate-risk zone as the region where the likelihood for no tipping event is smaller than 66% or the risk that one or more elements tip is higher than 33%. We compute this risk and find a marked increase for increasing convergence temperatures (compare Fig. 3d–f). For convergence temperatures of 1.5 °C and above, our results indicate that the high climate-risk zone spans the entire state space for final convergence temperatures of 1.5–2.0 °C. Only if final convergence temperatures are limited to or, better, below today's levels of global warming, while peak temperatures are below 3.0 °C, the tipping risks remain below

https://doi.org/10.1038/s41558-022-01545-9

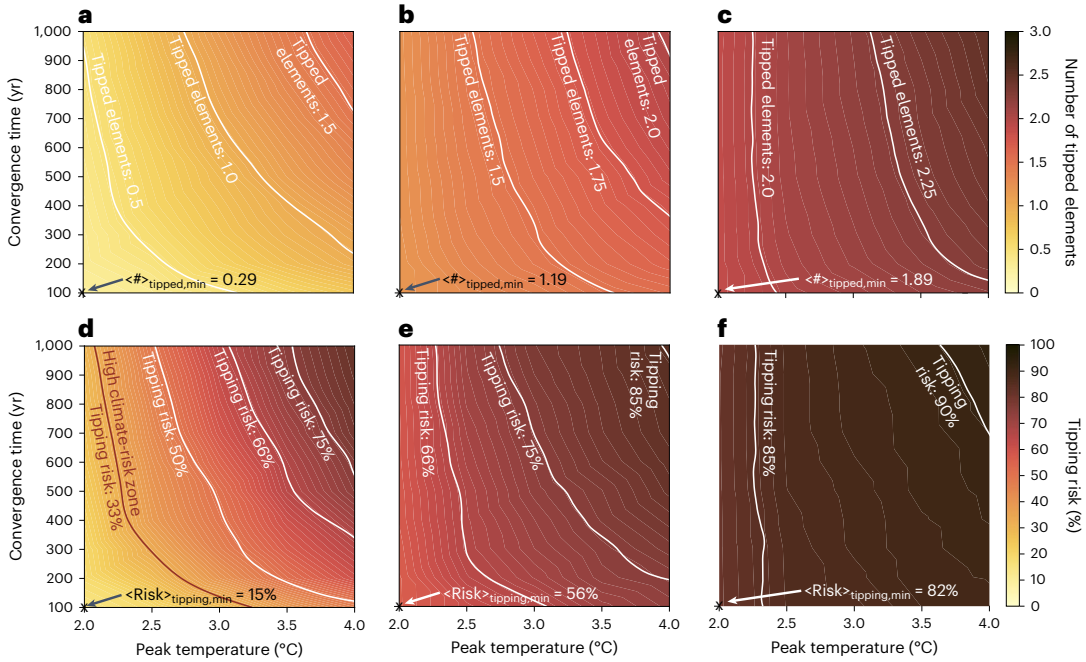

Fig. 3 | Expected number and risk of tipping events at different convergence temperatures. a, Number of tipped elements averaged over the entire ensemble for all investigated convergence times t_{Conv} and peak temperatures T_{Peak} at a convergence temperature of T_{Conv} = 1.0 °C above pre-industrial levels. The white lines show the conditions at which 0.5, 1.0 and 1.5 elements are tipped on average. $\langle\#\rangle_{tipped,min}$ is the average number of tipped elements at t_{Conv} = 100 yr and T_{Peak} = 2.0 °C. **b**,**c**, As in **a** but for convergence temperatures of 1.5 °C (**b**) and 2.0 °C (**c**). **d**, The risk that at least one tipping element transitions to its alternative state in equilibrium (after 50,000 simulation years) for a convergence temperature of 1.0 °C. The equipotential line in red indicates the high climate-risk zone (tipping risk is equal to 33%). $\langle Risk\rangle_{tipping,min}$ is the average risk of at least one element being tipped at t_{Conv} = 100 yr and T_{Peak} = 2.0 °C. **e**,**f**, As in **d** but for convergence temperatures of 1.5 °C (**e**) and 2.0 °C (**f**). The simulations for T_{Conv} = 0.0 °C (return to pre-industrial temperatures) and T_{Conv} = 0.5 °C can be found in Extended Data Fig. 4. High-end scenarios with T_{Peak} = 4.0–6.0 °C are added in Extended Data Figs. 5 and 6.

33% (Fig. 3d). In parallel, the equipotential lines shift strongly from higher peak temperatures and convergence times to lower ones with increasing convergence temperature. This leads to a lower likelihood of low-risk scenarios without tipping elements transitioning to their alternative state. In the worst case of a convergence temperature of 2.0 °C (Fig. 3f), the tipping risk for at least one tipping event to occur is on the order of above 90% if peak temperatures of 4.0 °C are not prevented. The devastating negative consequences of such a scenario with high likelihood of triggering tipping events would entail notable sea-level rise, biosphere degradation or considerable North Atlantic temperature drops.

Therefore, this would entail an unsafe overshoot regime. However, strictly lowering the final convergence temperature to or below today's levels of global warming while limiting peak overshoot temperatures to 3.0 °C and convergence times in parallel substantially reduces the risk of tipping events (Extended Data Fig. 4 and Fig. 3d). In the most optimistic scenario, tipping risks are kept below 5%.

Tipping mechanisms under warming overshoots

The risk for tipping events increases with higher peak temperatures, higher convergence temperatures and longer convergence times. However, the mechanism causing a tipping event in our model is twofold. (1) The element tips due to the final temperature T_{Conv} being higher than its critical temperature threshold. We call this baseline tipping because the final baseline (T_{Conv}) is already higher than the critical temperature (for example, Fig. 1a,b for the Greenland Ice Sheet). (2) The element tips due to the temperature overshoot trajectory, which temporarily transgresses its critical temperature threshold. We call this overshoot tipping (for example, Extended Data Fig. 1c for AMOC). In both cases, baseline tipping and overshoot tipping, the first tipped element can draw along other elements in a cascade such that the size of the cascade is not necessarily restricted to one. Our results show that the risk for tipping events in scenarios converging within the limits of the Paris climate target ranges from 57.8% to 91.4% (Fig. 4). For small peak temperatures (T_{Peak} = 2.5 °C), overshoot tipping accounts for as little as 9% of all tipping events, but for higher peak temperature levels (T_{Peak} = 4.0 °C), this number can increase to as much as 42% (bar charts in Fig. 3). Specifically, the risk of tipping increases 10–72% in these scenarios for overshooting before stabilizing at the convergence temperature as compared with non-overshoot scenarios. Note that in the special case where the peak temperature equals the convergence temperature ($T_{Peak} = T_{Conv}$ = 2.0 °C), overshoot tipping events do not occur.

The number of expected tipping events increases from short to long timescales as tested in our experiments, where we separated tipping events realized after 100 (short-term tipping), 1,000 (mid-term tipping) and 50,000 simulation years (equilibrium tipping; pie charts in Fig. 4). For higher peak temperatures, we additionally observe a larger portion of tipping events realized within 100 and 1,000 yr. These short-term events are dominantly caused by the fast-tipping elements (AMOC and Amazon rainforest), but mid-term events are also partially caused by a tipping West Antarctic Ice Sheet (Extended Data Fig. 2). Together, our results indicate that, to avoid tipping events within the Paris range, not only the peak temperature must be limited but also the final convergence temperature has to fall substantially below 1.5 °C in the long run (Fig. 3 and Extended Data Fig. 7). To further hedge tipping risks, the time to reach the convergence temperature must also be small ($t_{Conv} \lesssim$ 200 yr; compare Extended Data Fig. 4c,d). However, current policies and action would lead to 2.0–3.6 °C (mean: 2.7 °C), and present pledges and targets would lead to 1.7–2.6 °C (mean: 2.1 °C) above pre-industrial, according to the COP26 update published in November 2021 as expected temperatures in 2100 (see Climate Action Tracker and

https://doi.org/10.1038/s41558-022-01545-9

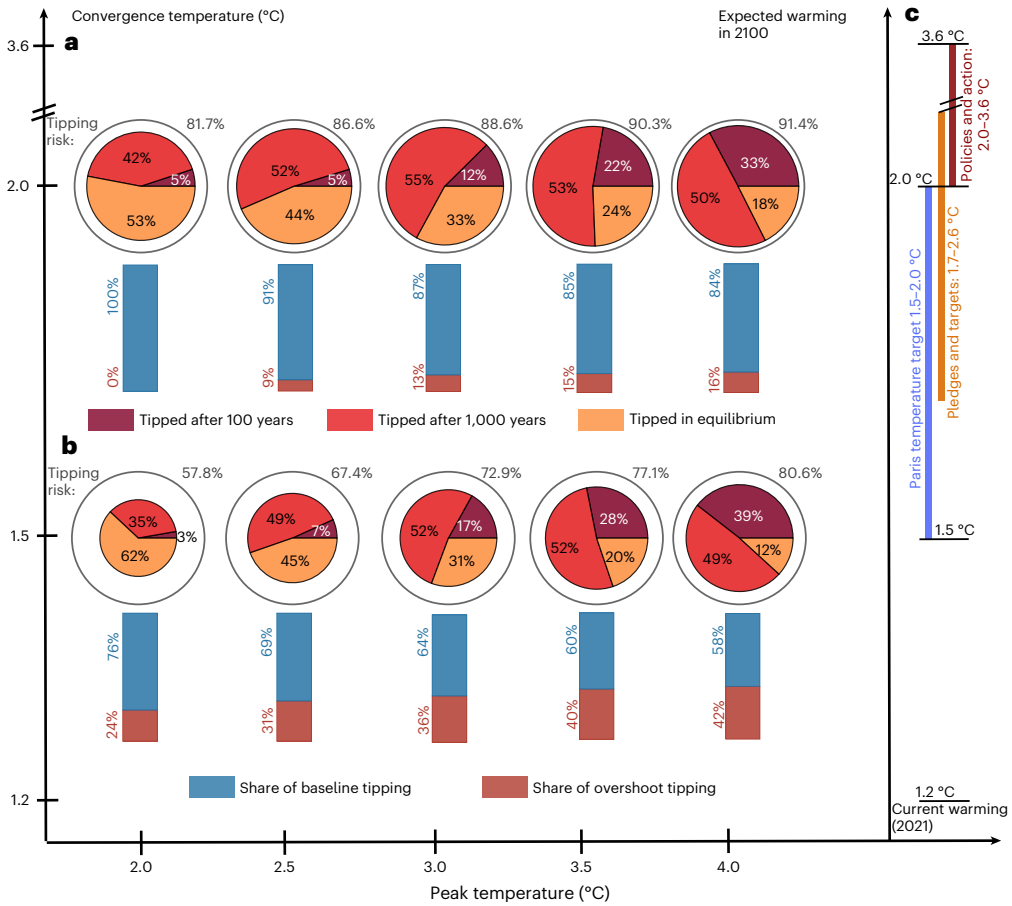

Fig. 4 | Timing and mechanisms of tipping events following temperature overshoots. Tipping risk with respect to overshoot scenarios of 2.0–4.0 °C and convergence temperatures within the Paris range of 1.5–2.0 °C above pre-industrial levels. The pie charts split the tipping events into the timescale when they occur: after 100 simulation years (dark red), after 1,000 simulation years (light red) or in equilibrium simulations (after 50,000 simulation years, orange). The size of the pie chart indicates the overall tipping risk (for example, 67.4% at T_{Conv} = 1.5 °C and T_{Peak} = 2.5 °C). The bar chart directly below the pie chart indicates the ratio between the two possible tipping mechanisms: (1) due to the convergence temperature being above the critical temperature for one or several tipping elements (baseline tipping, for an example see Greenland Ice Sheet in Extended Data Fig. 1d,e) and (2) due to the overshoot trajectory (overshoot tipping, for an example see AMOC in Extended Data Fig. 1c). **a**,**b**, Scenario where global mean temperature converges to 1.5 °C (**a**) or to 2.0 °C (**b**). **c**, Expected warming in 2100 after the COP26 pledges and targets (orange vertical line: 1.7–2.6 °C) and the policies and action (dark red vertical line: 2.0–3.6 °C) together with the current warming of 1.2 °C and the Paris temperature target (blue vertical line: 1.5–2.0 °C). Note that the vertical axes are nonlinear due to visibility. The data for the vertical lines have been compiled from the November 2021 update by Climate Action Tracker[14]. The scenarios with lower convergence temperatures of 0, 0.5 and 1.0 °C above pre-industrial are depicted in Extended Data Fig. 7. High-end climate scenarios and overshoots for peak temperatures between 4.5 and 6.0 °C are shown in Extended Data Fig. 8.

vertical axis in Fig. 4c)[14]. As noted, these temperatures would lead to notable tipping risks if they were interpreted as peak temperatures. If they would be convergence temperatures, tipping very likely is unavoidable. In addition, high-end scenario simulations with very high peak temperatures between 4.5 and 6.0 °C reveal that the risk to observe tipping becomes virtually certain (>95% for $T_{Peak} \gtrsim 5.5$ °C). At these scenarios, it is likely (>40%) that the first tipping event would occur within 100 yr, typically the Amazon rainforest or AMOC (Extended Data Fig. 8).

Furthermore, we investigate the effects of interactions between the tipping elements on the risk of (cascading) transitions in overshoot scenarios (Supplementary Section 2 and Supplementary Fig. 1). Our results show that increasing the interaction strength from 0 (no interaction) to 0.3 increases the average number of tipped elements strongly (by 49.3 ± 2.1%) at a convergence temperature of 2.0 °C. A further increase of the interaction strength from 0.3 leads to only a marginal additional tipping risk (of 12.1 ± 0.5%; Supplementary Fig. 1e).

Discussion

In summary, we find that in our stylized network model the high climate-risk zone characterized by large tipping risks (>33%) can be avoided only if several aspects are met in parallel due to the different timescales involved. These aspects are limited overshoot peak temperatures, limited convergence times and, most important, limited convergence temperatures (due to baseline tipping) to a level of or, better, below the current level of global warming (1.2 °C)[14]. Our model analysis shows that the overshoot peak temperature should be constrained on the basis of fast-tipping elements (Fig. 2b), whereas slow-tipping elements largely determine the upper limit for convergence times (Extended Data Fig. 3). The convergence temperature needs to be limited to avoid baseline tipping, and lower levels of it will also assist in avoiding overshoot tipping (Fig. 4). Therefore, the combination of the slow Greenland Ice Sheet having a low temperature threshold and the faster elements (AMOC, Amazon rainforest) having at least partially higher thresholds (Supplementary Table 1) facilitates the possibility of a small overshoot without causing tipping events and thus further cascades. Ritchie et al.[18] came to similar conclusions for individual tipping elements, but we find, for a sufficient interaction strength (≳0.2), a marked increase in the expected number of tipped elements in equilibrium due to the possibility of emerging tipping cascades (Supplementary Fig. 1). Taken together, safe and unsafe temporary overshoot trajectories can clearly be separated.

The choices of our stylized global warming overshoot scenarios are motivated by current knowledge, summarizing short- and long-term effects. The shape of the short-term overshoot trajectories captures the temperature profiles from different Earth system model simulations[42] but is still of a conceptualized nature (equation (2)). To allow for a direct comparison with the baseline critical temperatures, we keep the temperature trajectories at constant levels in the long run. While this is supported by Zero Emissions Commitment Model Intercomparison Project for the near to intermediate future for decades to centuries[43,44], it is unclear how carbon sinks and sources behave for the more distant future. On timescales of centuries to millennia, it seems more likely than not that a slight downward trend of global mean temperatures will be entered[44–46]. Still, large uncertainties remain and make future research necessary as has, for example, been proposed by using a novel framework of model experiments for zero emission simulations[47]. Overall, it is questionable whether naturally decreasing temperatures would be sufficient to bring global mean temperatures after an overshoot back down to safe levels without additional artificial carbon removal from the atmosphere[46].

Our employed stylized network model does not directly capture physical processes or the spatial extent of tipping elements (for example, important for spatial heterogeneity) and can as such not be used as a model for predictions, but it has been designed as a risk assessment tool for some of the potentially most nonlinear and societally harmful elements in the Earth system. Thus, a benefit of low-complexity models such as ours is that they allow for very large-scale Monte Carlo ensemble simulations, which can consider relevant uncertainties, for example, in interaction structure, strength and critical temperature thresholds. Still, future research should also be targeted at building more complex models around coupled nonlinear phenomena and climate tipping elements, either by combining simple physics-based models and combining those models with observational data[48–51] or by employing Earth system models of either intermediate or high complexity. In the latter case, tipping elements could be spatially resolved, which might refine or modify some of the results gained here[35]. Moreover, data-based approaches or machine learning should be considered, with which it might be possible to reconstruct actual interaction-strength values[17,52]. Recently, it has also been proposed to combine these two research strands to what has been framed 'neural' Earth system models[53]. In addition, uncertainty in the assumed fold-bifurcation structure should be considered in future work to probe how results would be affected if some of the tipping elements were less nonlinear, for example, due to spatial pattern formation or negative feedbacks[28,34,35]. Most important, this would decrease the abruptness of change expected in the model or may increase the time for complete disintegration of the respective (tipping) element. Thus, the convergence time for safe overshoots would probably be larger.

Even in the absence of climate tipping points, future climate change will cause high economic, ecological and societal damage; however, the need for climate action becomes even more urgent if (interacting) climate tipping elements would undergo a critical transition during an overshoot[54–56]. Critically, to reduce the risk and prevent the negative impacts of interacting climate tipping elements on human societies and biosphere integrity, it is of utmost importance to ensure that temperature overshoot trajectories are limited in both magnitude and duration, while stabilizing global warming at or, better, below the Paris Agreement's targets. Furthermore, also many of the low global-mean-temperature scenarios, limiting warming to well below 2 °C above pre-industrial levels, are forced to include an overshoot period over 1.5 °C (refs. 57,58). Our paper highlights the importance to investigate further the risks of triggering nonlinear changes also during these lower and shorter overshoots in future work. Although our results indicate that a future climate trajectory without or with limited temperature overshoots would be preferable, current results from the COP conferences and their pledges and targets indicate that at least temporary overshoots over the Paris range seem likely[14,59]. This would be problematic because of natural risks exerted by the potential of disintegrating climate tipping elements, but also, economic damages would be smaller in case of a non-overshoot scenario[59,60].

Online content

Any methods, additional references, Nature Portfolio reporting summaries, source data, extended data, supplementary information, acknowledgements, peer review information; details of author contributions and competing interests; and statements of data and code availability are available at https://doi.org/10.1038/s41558-022-01545-9.

References

1. Lenton, T. M. et al. Tipping elements in the Earth's climate system. *Proc. Natl Acad. Sci. USA* **105**, 1786–1793 (2008).
2. Schellnhuber, H. J. Tipping elements in the Earth System. *Proc. Natl Acad. Sci. USA* **106**, 20561–20563 (2009).
3. Steffen, W. et al. Trajectories of the Earth system in the Anthropocene. *Proc. Natl Acad. Sci. USA* **115**, 8252–8259 (2018).
4. Levermann, A. & Winkelmann, R. A simple equation for the melt elevation feedback of ice sheets. *Cryosphere* **10**, 1799–1807 (2016).
5. Aragão, L. E. The rainforest's water pump. *Nature* **489**, 217–218 (2012).
6. Armstrong McKay, D. I. et al. Exceeding 1.5 °C global warming could trigger multiple climate tipping points. *Science* **377**, eabn7950 (2022).
7. Schellnhuber, H. J., Rahmstorf, S. & Winkelmann, R. Why the right climate target was agreed in Paris. *Nat. Clim. Change* **6**, 649–653 (2016).
8. Garbe, J., Albrecht, T., Levermann, A., Donges, J. F. & Winkelmann, R. The hysteresis of the Antarctic ice sheet. *Nature* **585**, 538–544 (2020).
9. Robinson, A., Calov, R. & Ganopolski, A. Multistability and critical thresholds of the Greenland Ice Sheet. *Nat. Clim. Change* **2**, 429–432 (2012).
10. Hawkins, E. et al. Bistability of the Atlantic overturning circulation in a global climate model and links to ocean freshwater transport. *Geophys. Res. Lett.* **38** (2011).
11. Nobre, C. A. & Borma, L. D. S. 'Tipping points' for the Amazon forest. *Curr. Opin. Environ. Sustain.* **1**, 28–36 (2009).
12. Lenton, T. M. et al. Climate tipping points—too risky to bet against. *Nature* **575**, 592–595 (2019).
13. IPCC *Climate Change 2021: The Physical Science Basis* (eds Masson-Delmotte, V. P. et al.) (Cambridge Univ. Press, 2021).
14. *The CAT Thermometer* (Climate Analytics and New Climate Institute, 2021); https://climateactiontracker.org/global/cat-thermometer/
15. Meinshausen, M. et al. Realization of Paris Agreement pledges may limit warming just below 2 °C. *Nature* **604**, 304–309 (2022).
16. Schleussner, C.-F., Ganti, G., Rogelj, J. & Gidden, M. J. An emission pathway classification reflecting the Paris Agreement climate objectives. *Commun. Earth Environ.* **3**, 135 (2022).
17. Drijfhout, S. et al. Catalogue of abrupt shifts in Intergovernmental Panel on Climate Change climate models. *Proc. Natl Acad. Sci. USA* **112**, E5777–E5786 (2015).
18. Ritchie, P. D., Clarke, J. J., Cox, P. M. & Huntingford, C. Overshooting tipping point thresholds in a changing climate. *Nature* **592**, 517–523 (2021).
19. Tong, D. et al. Committed emissions from existing energy infrastructure jeopardize 1.5 °C climate target. *Nature* **572**, 373–377 (2019).
20. Raftery, A. E., Zimmer, A., Frierson, D. M., Startz, R. & Liu, P. Less than 2 °C warming by 2100 unlikely. *Nat. Clim. Change* **7**, 637–641 (2017).
21. Ritchie, P., Karabacak, Ö. & Sieber, J. Inverse-square law between time and amplitude for crossing tipping thresholds. *Proc. R. Soc. A* **475**, 20180504 (2019).

22. Alkhayuon, H., Ashwin, P., Jackson, L. C., Quinn, C. & Wood, R. A. Basin bifurcations, oscillatory instability and rate-induced thresholds for Atlantic meridional overturning circulation in a global oceanic box model. *Proc. R. Soc. A* **475**, 20190051 (2019).
23. Rocha, J. C., Peterson, G., Bodin, Ö. & Levin, S. Cascading regime shifts within and across scales. *Science* **362**, 1379–1383 (2018).
24. Lenton, T. M. & Williams, H. T. On the origin of planetary-scale tipping points. *Trends Ecol. Evol.* **28**, 380–382 (2013).
25. Kriegler, E., Hall, J. W., Held, H., Dawson, R. & Schellnhuber, H. J. Imprecise probability assessment of tipping points in the climate system. *Proc. Natl Acad. Sci. USA* **106**, 5041–5046 (2009).
26. Wunderling, N., Donges, J. F., Kurths, J. & Winkelmann, R. Interacting tipping elements increase risk of climate domino effects under global warming. *Earth Syst. Dyn.* **12**, 601–619 (2021).
27. Bathiany, S. et al. Beyond bifurcation: using complex models to understand and predict abrupt climate change. *Dynamics Stat. Clim. Syst.* **1**, 1–31 (2016).
28. Goosse, H. et al. Quantifying climate feedbacks in polar regions. *Nat. Commun.* **9**, 1919 (2018).
29. Soden, B. J. & Held, I. M. An assessment of climate feedbacks in coupled ocean–atmosphere models. *J. Clim.* **19**, 3354–3360 (2006).
30. Lucarini, V. & Bódai, T. Transitions across melancholia states in a climate model: reconciling the deterministic and stochastic points of view. *Phys. Rev. Lett.* **122**, 158701 (2019).
31. Margazoglou, G., Grafke, T., Laio, A. & Lucarini, V. Dynamical landscape and multistability of a climate model. *Proc. R. Soc. A* **477**, 20210019 (2021).
32. Wunderling, N., Willeit, M., Donges, J. F. & Winkelmann, R. Global warming due to loss of large ice masses and Arctic summer sea ice. *Nat. Commun.* **11**, 5177 (2020).
33. Boulton, C. A., Lenton, T. M. & Boers, N. Pronounced loss of Amazon rainforest resilience since the early 2000s. *Nat. Clim. Change* **12**, 271–278 (2022).
34. Bastiaansen, R., Dijkstra, H. A. & von der Heydt, A. S. Fragmented tipping in a spatially heterogeneous world. *Environ. Res. Lett.* **17**, 045006 (2022).
35. Rietkerk, M. et al. Evasion of tipping in complex systems through spatial pattern formation. *Science* **374**, eabj0359 (2021).
36. Wunderling, N. et al. Recurrent droughts increase risk of cascading tipping events by outpacing adaptive capacities in the Amazon rainforest. *Proc. Natl Acad. Sci. USA* **119**, e2120777119 (2022).
37. Kemp, L. et al. Climate endgame: exploring catastrophic climate change scenarios. *Proc. Natl Acad. Sci. USA* **119**, e2108146119 (2022).
38. Jehn, F. U. et al. Focus of the IPCC assessment reports has shifted to lower temperatures. *Earths Future* **10**, e2022EF002876 (2022).
39. Weijer, W. et al. Stability of the Atlantic meridional overturning circulation: a review and synthesis. *J. Geophys. Res. Oceans* **124**, 5336–5375 (2019).
40. Jackson, L. et al. Global and European climate impacts of a slowdown of the AMOC in a high resolution GCM. *Clim. Dyn.* **45**, 3299–3316 (2015).
41. Mitrovica, J. X., Gomez, N. & Clark, P. U. The sea-level fingerprint of West Antarctic collapse. *Science* **323**, 753 (2009).
42. Huntingford, C. et al. Flexible parameter-sparse global temperature time profiles that stabilise at 1.5 and 2.0 °C. *Earth Syst. Dyn.* **8**, 617–626 (2017).
43. Jones, C. D. et al. The Zero Emissions Commitment Model Intercomparison Project (ZECMIP) contribution to C4MIP: quantifying committed climate changes following zero carbon emissions. *Geosci. Model Dev.* **12**, 4375–4385 (2019).
44. MacDougall, A. H. et al. Is there warming in the pipeline? A multi-model analysis of the Zero Emissions Commitment from CO_2. *Biogeosciences* **17**, 2987–3016 (2020).
45. Williams, R. G., Roussenov, V., Frölicher, T. L. & Goodwin, P. Drivers of continued surface warming after cessation of carbon emissions. *Geophys. Res. Lett.* **44**, 10633–10642 (2017).
46. Zickfeld, K. et al. Long-term climate change commitment and reversibility: an EMIC intercomparison. *J. Clim.* **26**, 5782–5809 (2013).
47. King, A. D. et al. Studying climate stabilization at Paris Agreement levels. *Nat. Clim. Change* **11**, 1010–1013 (2021).
48. Dekker, M. M., Von Der Heydt, A. S. & Dijkstra, H. A. Cascading transitions in the climate system. *Earth Syst. Dyn.* **9**, 1243–1260 (2018).
49. Ciemer, C., Winkelmann, R., Kurths, J. & Boers, N. Impact of an AMOC weakening on the stability of the southern Amazon rainforest. *Eur. Phys. J. Spec. Top.* **230**, 3065–3073 (2021).
50. Lohmann, J. & Ditlevsen, P. D. Risk of tipping the overturning circulation due to increasing rates of ice melt. *Proc. Natl Acad.Sci. USA*. **118**, e2017989118 (2021).
51. Sinet, S., Dijkstra, H. A. & von der Heydt, A. S. AMOC stabilization under the interaction with tipping polar ice sheets. Preprint at *ESSOAr* https://doi.org/10.1002/essoar.10511833.1 (2022).
52. Runge, J. et al. Identifying causal gateways and mediators in complex spatio-temporal systems. *Nat. Commun.* **6**, 8502 (2015).
53. Irrgang, C. et al. Towards neural Earth system modelling by integrating artificial intelligence in Earth system science. *Nat. Mach. Intell.* **3**, 667–674 (2021).
54. Cai, Y., Lenton, T. M. & Lontzek, T. S. Risk of multiple interacting tipping points should encourage rapid CO_2 emission reduction. *Nat. Clim. Change* **6**, 520–525 (2016).
55. Cai, Y., Judd, K. L., Lenton, T. M., Lontzek, T. S. & Narita, D. Environmental tipping points significantly affect the cost-benefit assessment of climate policies. *Proc. Natl Acad. Sci. USA* **112**, 4606–4611 (2015).
56. Lemoine, D. & Traeger, C. P. Economics of tipping the climate dominoes. *Nat. Clim. Change* **6**, 514–519 (2016).
57. IPCC *Special Report on Global Warming of 1.5 °C* (eds Masson-Delmotte, V. et al.) (Cambridge Univ. Press, 2018).
58. Schleussner, C.-F. et al. Science and policy characteristics of the Paris Agreement temperature goal. *Nat. Clim. Change* **6**, 827–835 (2016).
59. Drouet, L. et al. Net zero-emission pathways reduce the physical and economic risks of climate change. *Nat. Clim. Change* **11**, 1070–1076 (2021).
60. Riahi, K. et al. Cost and attainability of meeting stringent climate targets without overshoot. *Nat. Clim. Change* **11**, 1063–1069 (2021).
61. Elson, P. et al. Cartopy: a cartographic python library with a matplotlib interface. *Zenodo* https://doi.org/10.5281/zenodo.7065949 (2022).

Methods

Interacting climate tipping-elements model

We use the stylized network model designed for risk analysis of four interacting tipping elements detailed in ref. 26. Each tipping element is described by the following differential equation

$$\frac{\mathrm{d}x_i}{\mathrm{d}t} = \left[-x_i^3 + x_i + \sqrt{\frac{4}{27}} \times \frac{\Delta\mathrm{GMT}(t)}{T_{\mathrm{crit},i}} + d \times \sum_{\substack{j \\ j \neq i}} \frac{s_{ij}}{10}(x_j + 1) \right] \frac{1}{\tau_i} \quad (1)$$

Here, x_i describes the state of the respective tipping element i = Greenland Ice Sheet; AMOC; West Antarctic Ice Sheet (WAIS); Amazon rainforest (AMAZ). This differential equation possesses two different stable states: a baseline regime around $x_i \approx -1.0$ and a transitioned regime around $x_i \approx +1.0$. $\Delta\mathrm{GMT}(t)$ denotes the global mean surface temperature increase above pre-industrial levels (as compared with the 1850–1900 level). This term is time dependent because of the time dependence of the overshoot trajectory, which serves as our input: $\Delta\mathrm{GMT}(t)$ = overshoot trajectory(t). The mathematical form of the overshoot trajectory is given in Temperature overshoot trajectories. $T_{\mathrm{crit},i}$ denotes the critical temperatures for the four tipping elements. The link strength values s_{ij} are taken from an expert elicitation[25], and each represents a physical mechanism (Fig. 1c and Supplementary Table 1). While these link strength values are quantified, the absolute importance of the interaction is not known for many of the interactions. Therefore, we introduce the interaction-strength parameter d, which is varied between 0 and 1.0, where $d = 0$ means no interaction between the tipping elements and $d = 1.0$ means that interactions are approximately as important as the individual dynamics. With that we can probe a large range of possible interaction strengths among the tipping elements.

Last, the timescale parameter τ_i denotes the transition time of a particular tipping element. Of course, the four stylized differential equations (equation (1)) are a strong simplification of the more complex tipping elements. However, they represent a summary of the main stability patterns, as has been argued in literature before[26,27]. For more details on the mathematics in this model, refer to ref. 26. As initial conditions at $t = 0$, the states of the four climate tipping elements are set to $x_i = -1.0$ (the completely untipped baseline regime), and the parameters for T_{crit}, s_{ij} and τ_{i} are chosen from their respective limits (Parameter uncertainties and Supplementary Table 1).

Parameter uncertainties

There are uncertainties in several parameters of the model (equation (1) and Supplementary Table 1). (1) The critical temperature regimes $T_{\mathrm{crit},i}$ are taken from the recently refined literature values[6]. (2) The interactions between the climate tipping elements all represent physical mechanisms behind each pair of tipping elements. For example, a melting Greenland Ice Sheet induces a freshwater input into the North Atlantic and, by that, weakens the AMOC, while a weakening AMOC would reduce the warming over Greenland (Fig. 1). There is a considerable uncertainty of the link strength parameters s_{ij}, which are included in our uncertainty analysis, and their values are taken from an expert elicitation on interacting climate tipping elements[25]. The same values for interaction strengths have been used in earlier research on tipping cascades[26]. (3) The upper and lower bounds for transition times for the four tipping elements are again taken from recent literature[6]. It is important to note that the timescales for tipping vary from decades, over centuries up to millennia depending on the respective tipping element. While the Amazon rainforest and the AMOC tip on shorter timescales (decades to centuries), the Greenland and West Antarctic ice sheets take longer to disintegrate (multiple centuries to millennia). These, on at least two orders of magnitude, different transition times have important effects on the dynamics of tipping and as to whether a specific tipping event occurs or not. These effects are discussed in the main text.

Propagation of uncertainties via a Monte Carlo ensemble

Since there are considerable uncertainties in the critical temperature regimes, interaction strengths and structure, as well as in the transition timescales, we set up a large-scale Monte Carlo ensemble to adequately propagate the uncertainties in these parameters. The uncertainty ranges of the parameter uncertainties are given in Supplementary Table 1. For each combination of peak temperature ($T_{\mathrm{Peak}} = 2.0, 2.5, \ldots, 6.0$ °C), convergence temperature ($T_{\mathrm{Conv}} = 0.0, 0.5, \ldots, 2.0$ °C), convergence time ($t_{\mathrm{Conv}} = 100, 200, \ldots, 1{,}000$ yr) and interaction strength ($d = 0.0, 0.1, \ldots, 1.0$), we draw 100 realizations from a continuous uniform distribution using a Latin hypercube algorithm[62] over the uncertainties in critical temperatures, link strengths and transition times. This leads to $9 \times 5 \times 10 \times 11 \times 100 = 495{,}000$ ensemble members, which are looped over the nine possible different network structures ((1) a positive link from WAIS to AMOC and a positive link from AMOC to AMAZ, (2) a zero link from WAIS to AMOC and a positive link from AMOC to AMAZ, ..., (9) a negative link from WAIS to AMOC and a negative link from AMOC to AMAZ). With this procedure, we obtain approximately 4.455 million ensemble members in total. By drawing from a continuous uniform distribution for all tipping elements, we slightly overestimate the overall uncertainties and perform a maximum uncertainty assessment. Therefore, our errors are conservative. After 100 yr, after 1,000 yr and in equilibrium (here, 50,000 yr), we branch off the results for each of our 4.455 million ensemble members such that we can assess our results at these three different timings.

Temperature overshoot trajectories

In this study, we have used stylized temperature overshoot trajectories based on overshoot trajectories that capture temperature profiles generated by Earth system model simulations for a low- to medium-emissions scenario[42]:

$$\Delta\mathrm{GMT}(t) = T_0 + \gamma t - \left[1 - e^{-(\mu_0 + \mu_1 t)t}\right][\gamma t - (T_{\mathrm{Conv}} - T_0)] \quad (2)$$

In this equation, the temperature overshoot trajectory $\Delta\mathrm{GMT}(t)$ is determined via five parameters. (1) T_0 is the approximate current level of global warming, that is, the point at which the trajectories start at $t = 0$. We have chosen $T_0 = 1.0$ °C above pre-industrial levels. (2) T_{Conv} is the final convergence temperature, for which we have chosen an ensemble approach comprising $T_{\mathrm{Conv}} = 0, 0.5, 1.0, 1.5, 2.0$ °C above pre-industrial. (3) The parameter γ is chosen such that the global warming rate matches the recent past. The exponential decay term describes the development away from the linearly increasing trend (set by γ) bent towards the stabilization level (set by T_{Conv}), specified by the parameters (4) μ_0 and (5) μ_1. In our ensemble, we construct a temperature overshoot trajectory with a specific peak temperature T_{Peak} and convergence time t_{Conv} by iteratively altering the parameters γ, μ_0 and μ_1 until it matches the desired peak temperature and convergence time. Exemplary overshoot trajectories can be found in Extended Data Fig. 1, where the chosen parameters correspond to Fig. 1a. The chosen parameter values to get $T_{\mathrm{Peak}} = 2.5$ °C and $t_{\mathrm{Conv}} = 400$ yr are $\gamma = 0.0963$ °C yr^{-1}, $\mu_0 = 1.5 \times 10^{-3}$ yr^{-1} and $\mu_1 = 1.83 \times 10^{-4}$ yr^{-2}. The convergence temperature is set to $T_{\mathrm{Conv}} = 2.0$ °C. The accuracy we require for our scenarios is $\Delta T_{\mathrm{Peak}} < 0.025$ °C and $\Delta t_{\mathrm{Conv}} < 0.5$ yr, where the convergence time is determined as the time when the temperature overshoot curve has reached the convergence temperature to an accuracy of 0.01 °C.

Notes on maps

This paper makes use of perceptually uniform colour maps developed by F. Crameri[63].

Data availability

The data on overshoot trajectories and time series of the 4.455 million individual ensemble members are, due to the very high storage requirements, available from N.W. upon reasonable request.

Code availability

The code leading to the overshoot trajectories and tipping-risk assessments is available within the python modelling package pycascades at https://pypi.org/project/pycascades/, together with a model description paper[64]. The version of pycascades of the results of this manuscript is stored together with a readme, code of the figure files and intermediate evaluation scripts via https://doi.org/10.6084/m9.figshare.21408243. In case of questions or requests, please contact N.W.

References

62. Baudin, M. pyDOE: the experimental design package for python https://pythonhosted.org/pyDOE/index.html (2013).
63. Crameri, F. Geodynamic diagnostics, scientific visualisation and staglab 3.0. *Geosci. Model Dev.* **11**, 2541–2562 (2018).
64. Wunderling, N. et al. Modelling nonlinear dynamics of interacting tipping elements on complex networks: the PyCascades package. *Eur. Phys. J. Spec. Top.* **230**, 3163–3176 (2021).

Acknowledgements

This work has been carried out within the framework of PIK's FutureLab on Earth Resilience in the Anthropocene. N.W., J.R. and J.F.D. acknowledge support from the European Research Council Advanced Grant project ERA (Earth Resilience in the Anthropocene, ERC-2016-ADG-743080). J.F.D. is grateful for financial support by the project CHANGES funded by the Federal Ministry for Education and Research (BMBF) within the framework 'PIK_Change' under grant 01LS2001A. R.W., J.R., D.I.A.M., S.L. and B.S. acknowledge financial support via the Earth Commission, hosted by FutureEarth. The Earth Commission is the science component of the Global Commons Alliance, a sponsored project of Rockefeller Philanthropy Advisors, with support from Oak Foundation, MAVA, Porticus, Gordon and Betty Moore Foundation, Herlin Foundation and the Global Environment Facility. The Earth Commission is also supported by the Global Challenges Foundation. P.D.L.R. acknowledges support from the European Research Council 'Emergent Constraints on Climate–Land feedbacks in the Earth System (ECCLES)' project, grant agreement number 742472. The authors gratefully acknowledge the European Regional Development Fund (ERDF), the BMBF and the Land Brandenburg for supporting this project by providing resources on the high-performance computer system at the Potsdam Institute for Climate Impact Research.

Author contributions

R.W., J.R. and J.F.D. conceived the study. N.W. designed the study, performed the simulations and led the writing of the manuscript with input from all authors. N.W., S.L. and B.S. prepared the figures with input from R.W., J.R., P.D.L.R., D.I.A.M., and J.F.D. J.F.D. led the supervision of this study.

Competing interests

The authors declare no competing interests.

Additional information

Extended data is available for this paper at https://doi.org/10.1038/s41558-022-01545-9.

Supplementary information The online version contains supplementary material available at https://doi.org/10.1038/s41558-022-01545-9.

Correspondence and requests for materials should be addressed to Nico Wunderling or Jonathan F. Donges.

Peer review information *Nature Climate Change* thanks Max Rietkerk, Bregje van der Bolt and the other, anonymous, reviewer(s) for their contribution to the peer review of this work.

https://doi.org/10.1038/s41558-022-01545-9

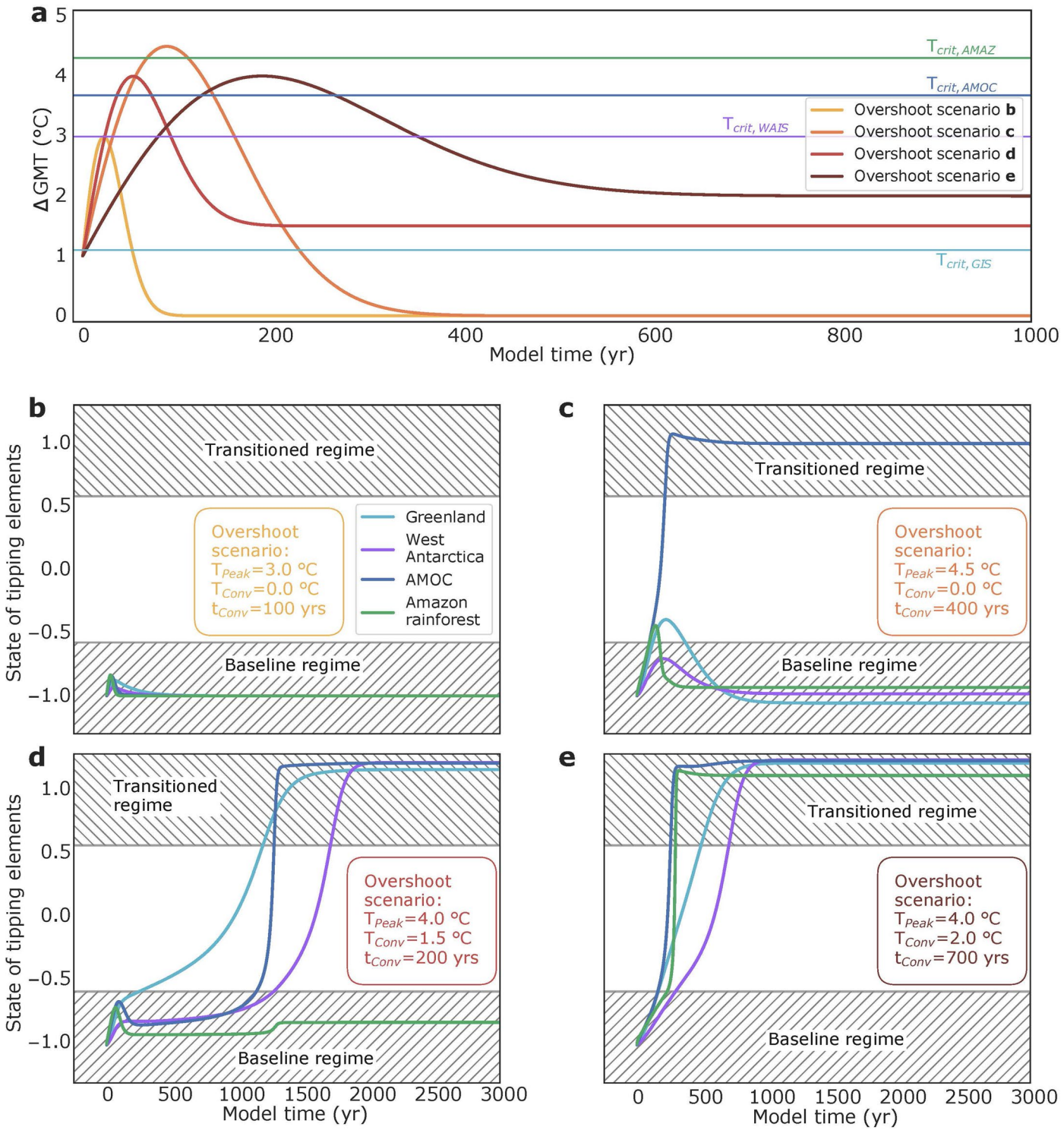

Extended Data Fig. 1 | Exemplary overshoot trajectories and their impact on tipping events. a, Time series of four different exemplary overshoot trajectories in dependence of the global mean surface temperature increase above pre-industrial levels (ΔGMT). Additionally, the four horizontal coloured lines show the critical temperatures of the Greenland Ice Sheet (GIS), the West Antarctic Ice Sheet (WAIS), the AMOC and the Amazon rainforest (AMAZ) for this specific ensemble member (for the entire ensemble of overshoots and tipping element set-ups, see Methods). **b-d**, The impact on tipping events in response to the applied overshoot scenario. Even though we only show one exemplary ensemble member here, it is apparent that higher temperature stabilisation levels (T_Conv) lead to a higher number of tipped elements (compare scenarios in **b, c** with scenarios in **d, e**), but also higher peak temperatures and convergence times have the same effect. The parameter values for this example are (same as in Fig. 1a,b): T_crit,GIS=1.1°C, T_crit,AMOC=3.6°C, T_crit,WAIS=3.0°C, T_crit,AMAZ=4.3°C, s_GIS → AMOC=9.2, s_AMOC → GIS=-3.1, s_GIS → AMOC=9.5, s_WAIS → AMOC=1.1, s_WAIS → GIS=1.5, s_GIS → WAIS=1.5, s_AMOC → AMAZ=3.0, τ_GIS=1602 yrs, τ_AMOC=172 yrs, τ_WAIS=1008 yrs and τ_AMAZ=56 yrs. The interaction strength parameter is set to d=0.20. For more details on the parameter values and meaning, see Methods.

https://doi.org/10.1038/s41558-022-01545-9

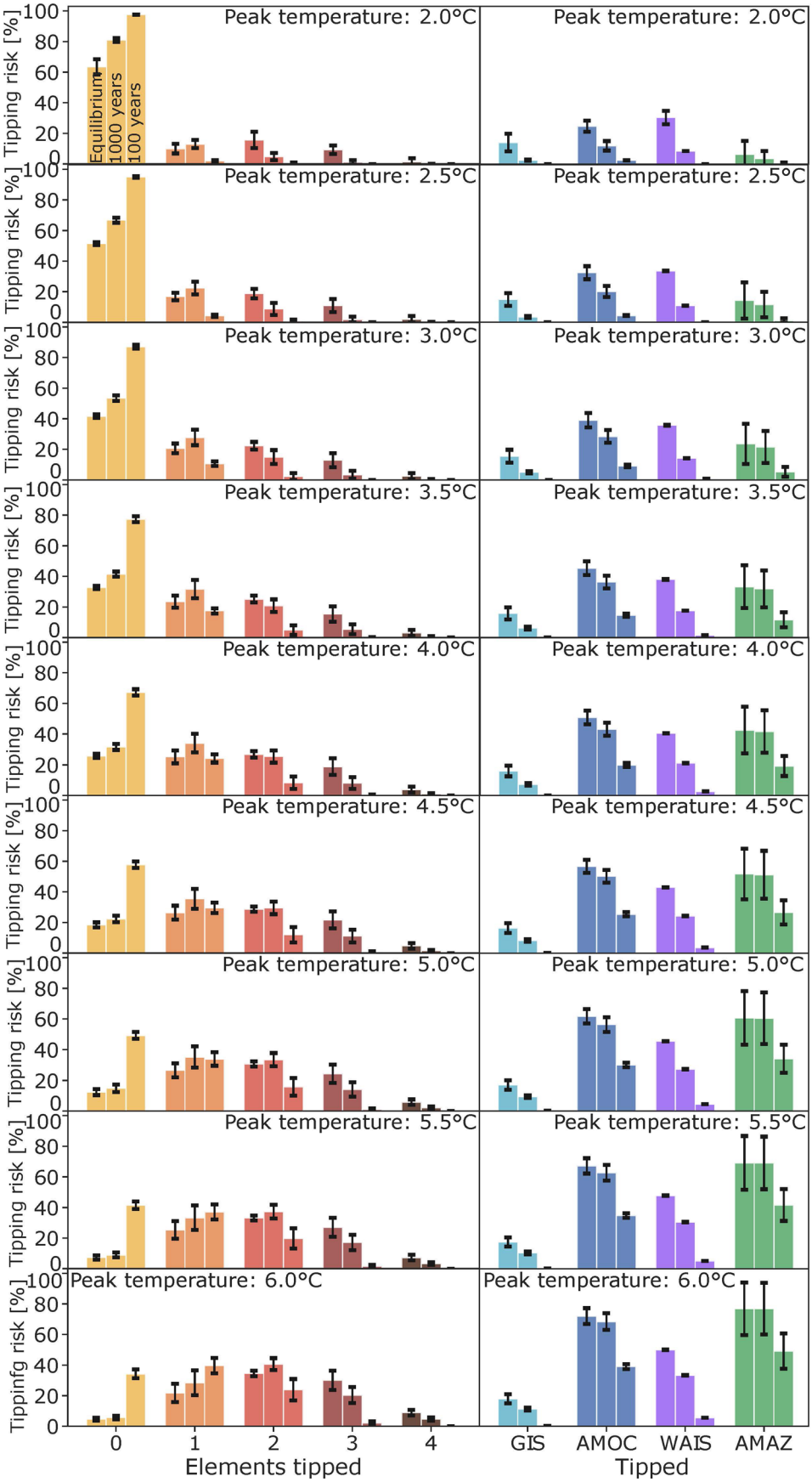

Extended Data Fig. 2 | See next page for caption.

https://doi.org/10.1038/s41558-022-01545-9

Extended Data Fig. 2 | The effect of time scales in overshoot scenarios on the risk for tipping events. In the left column, the probability of zero, one, two, three, or four tipped elements are shown for peak temperatures between T_Peak=2.0°C (lowest scenario) up to T_Peak=6.0°C (highest scenario). The right column breaks down the respective elements, which are responsible for the respective average number of tipped elements from the left column. The three parallel drawn bars in each panel detail the time scale of tipping into three scenarios. The left bar shows the result in equilibrium simulations (after 50,000 simulation years, long-term tipping), the bar in the middle shows the tipping events after 1,000 simulation years (mid-term tipping), and the right bar after 100 simulation years (short-term tipping). We depict the average over the entire ensemble as the bar height and the error bars show the standard deviation.

https://doi.org/10.1038/s41558-022-01545-9

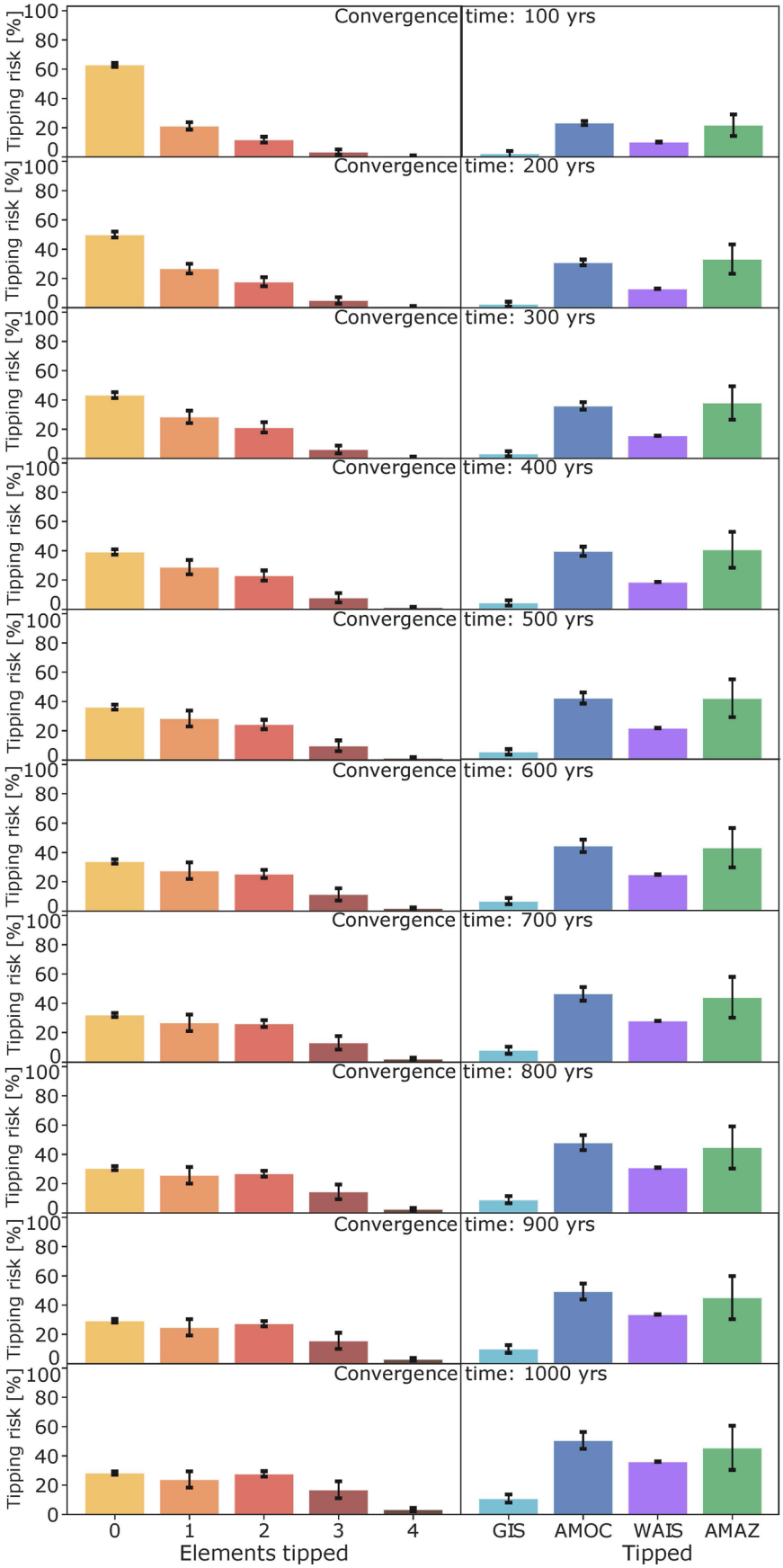

Extended Data Fig. 3 | The effect of the convergence time on the risk for tipping events. In the left column, the probability of zero, one, two, three, or four tipped elements are shown for convergence times of t_Conv=100 years (uppermost row) up to t_Conv=1,000 years (lowermost row). The right column breaks down the respective elements, which are responsible for the respective average number of tipped elements from the left column. We depict the average of the equilibrium run (long-term tipping after 50,000 simulation years) over the entire ensemble as the bar height and the error bars show the standard deviation.

https://doi.org/10.1038/s41558-022-01545-9

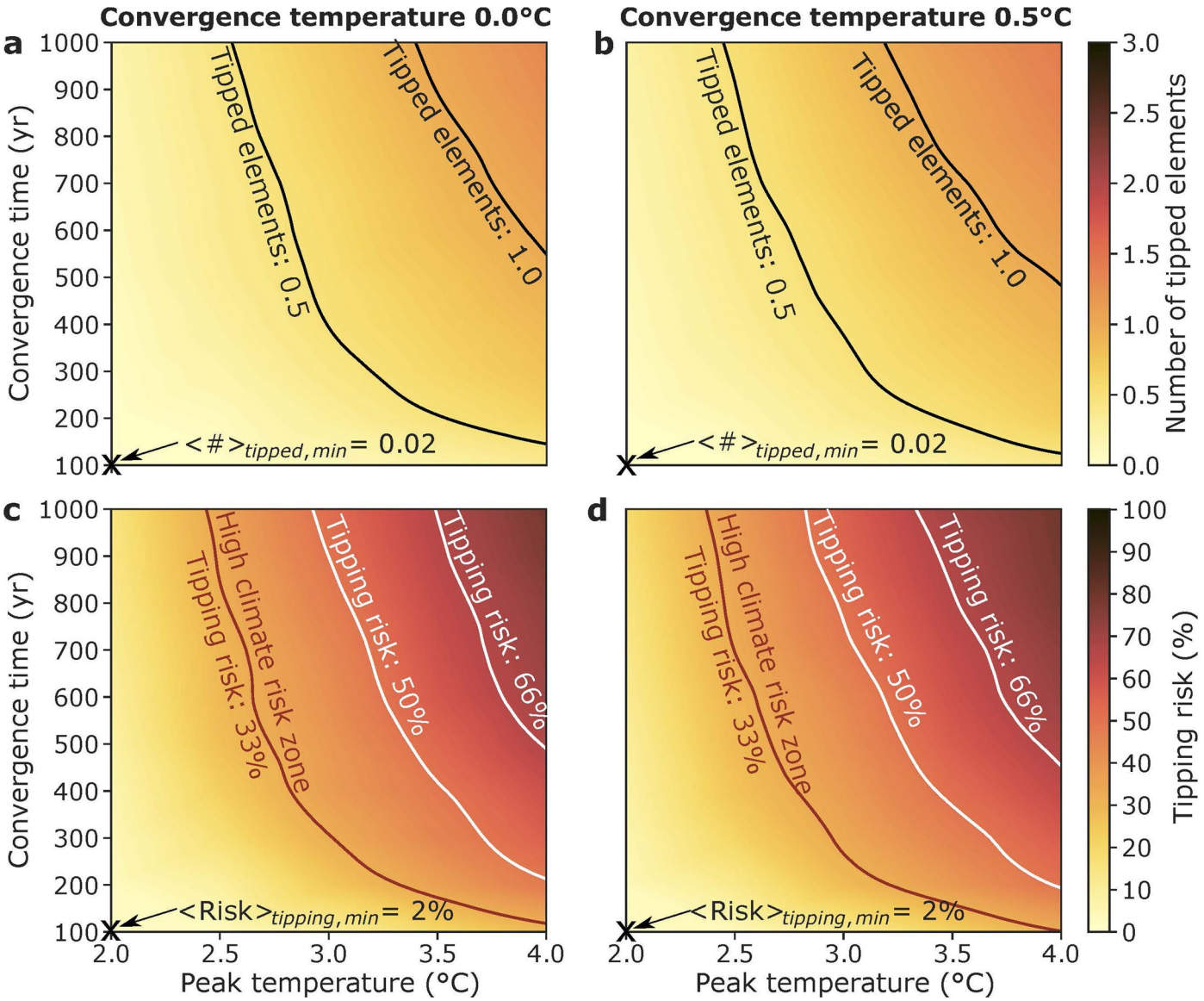

Extended Data Fig. 4 | Expected number and risk of tipping events at low convergence temperatures. Same as in Fig. 3 in the main manuscript, where the average number of tipped elements is shown for a set of convergence times and peak temperatures at a convergence temperature of **a**, 0.0°C (return to pre-industrial levels) and **b**, 0.5°C. The respective tipping risk that at least one tipping element ends up in the tipped regime is shown in panels **c, d**. Note that the *high climate risk zone* commences at higher peak and convergence times as compared to Fig. 3d in the main manuscript.

https://doi.org/10.1038/s41558-022-01545-9

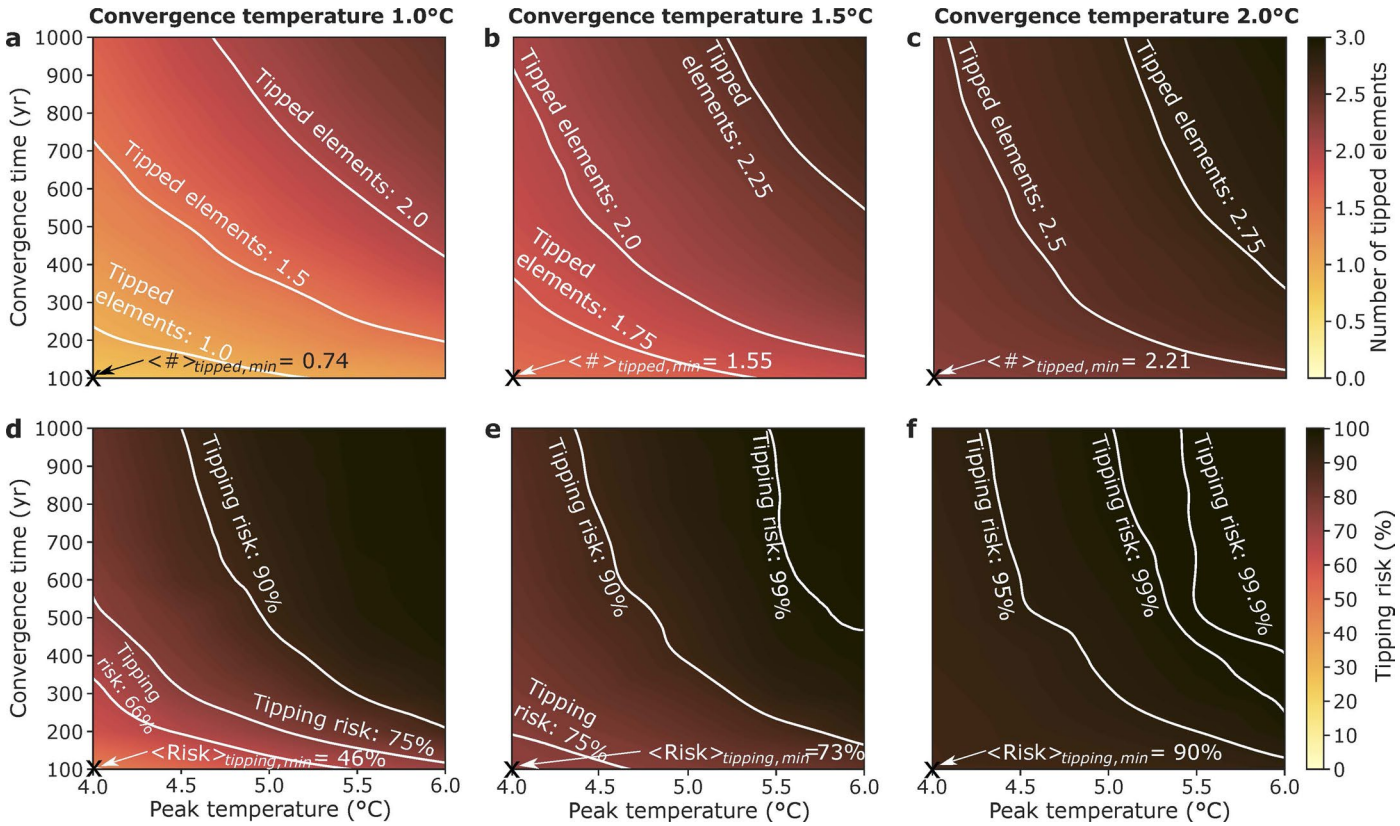

Extended Data Fig. 5 | Expected number and risk of tipping events for high-end temperature overshoots. Same as in Fig. 3 in the main manuscript, where the average number of tipped elements is shown for a set of convergence times and peak temperatures at a convergence temperature of **a**, 1.0°C, **b**, 1.5°C, and **c**, 2.0°C. The respective tipping risk that at least one tipping element ends up in the tipped regime is shown in panels **d, e, f**. For all high-end scenarios, the tipping risk for one tipping event to occur ~ 75% if final convergence temperatures are between 1.5 – 2. 0°C above pre-industrial levels.

https://doi.org/10.1038/s41558-022-01545-9

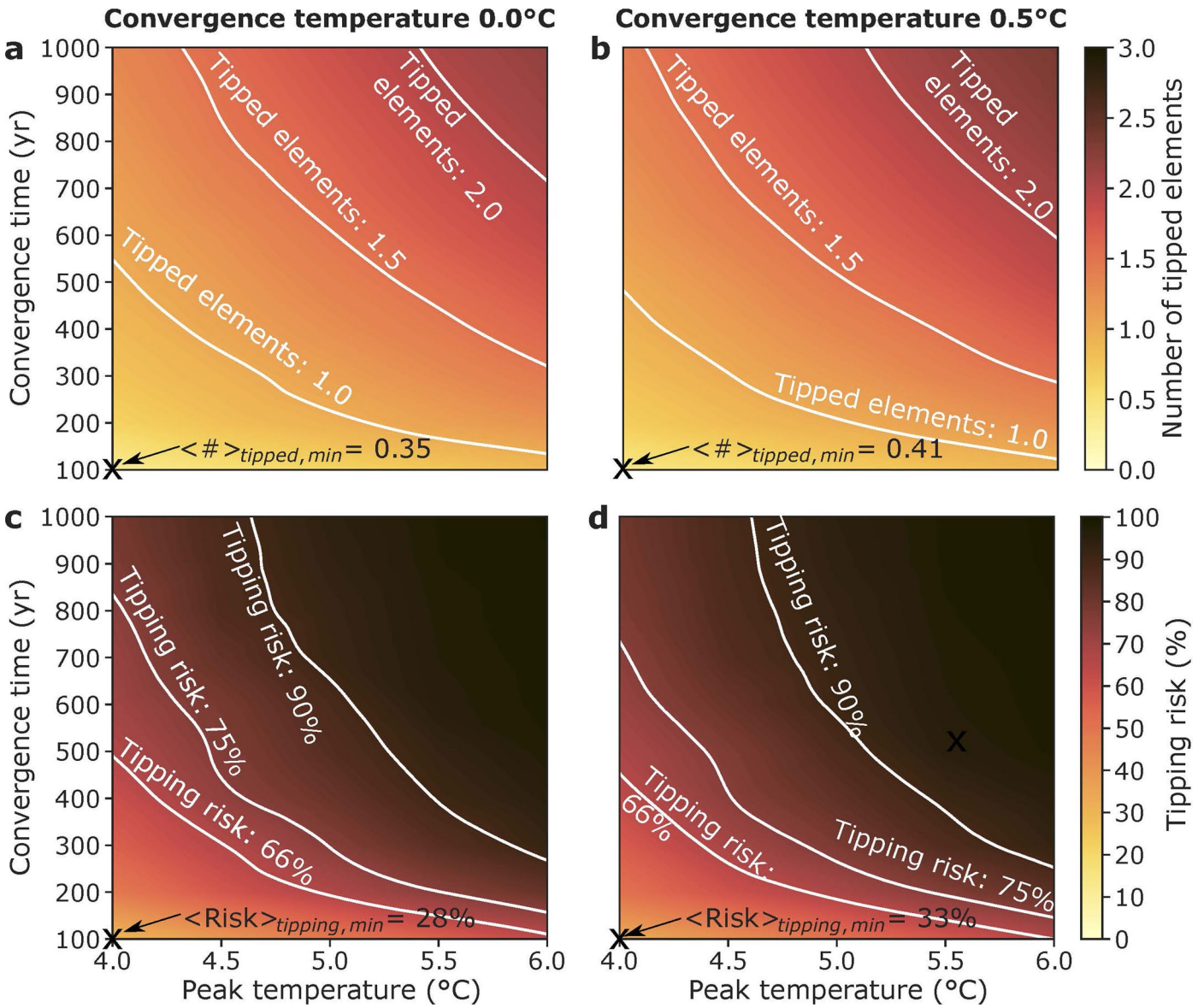

Extended Data Fig. 6 | Expected number and risk of tipping events for high-end temperature overshoots at low convergence temperatures. Same as in Extended Data Fig. 3, where the average number of tipped elements is shown for a set of convergence times and peak temperatures at a convergence temperature of **a**, 0.0°C (return to pre-industrial levels) and **b**, 0.5°C. The respective tippivng risk that at least one tipping element ends up in the tipped regime is shown in panels **c, d**.

https://doi.org/10.1038/s41558-022-01545-9

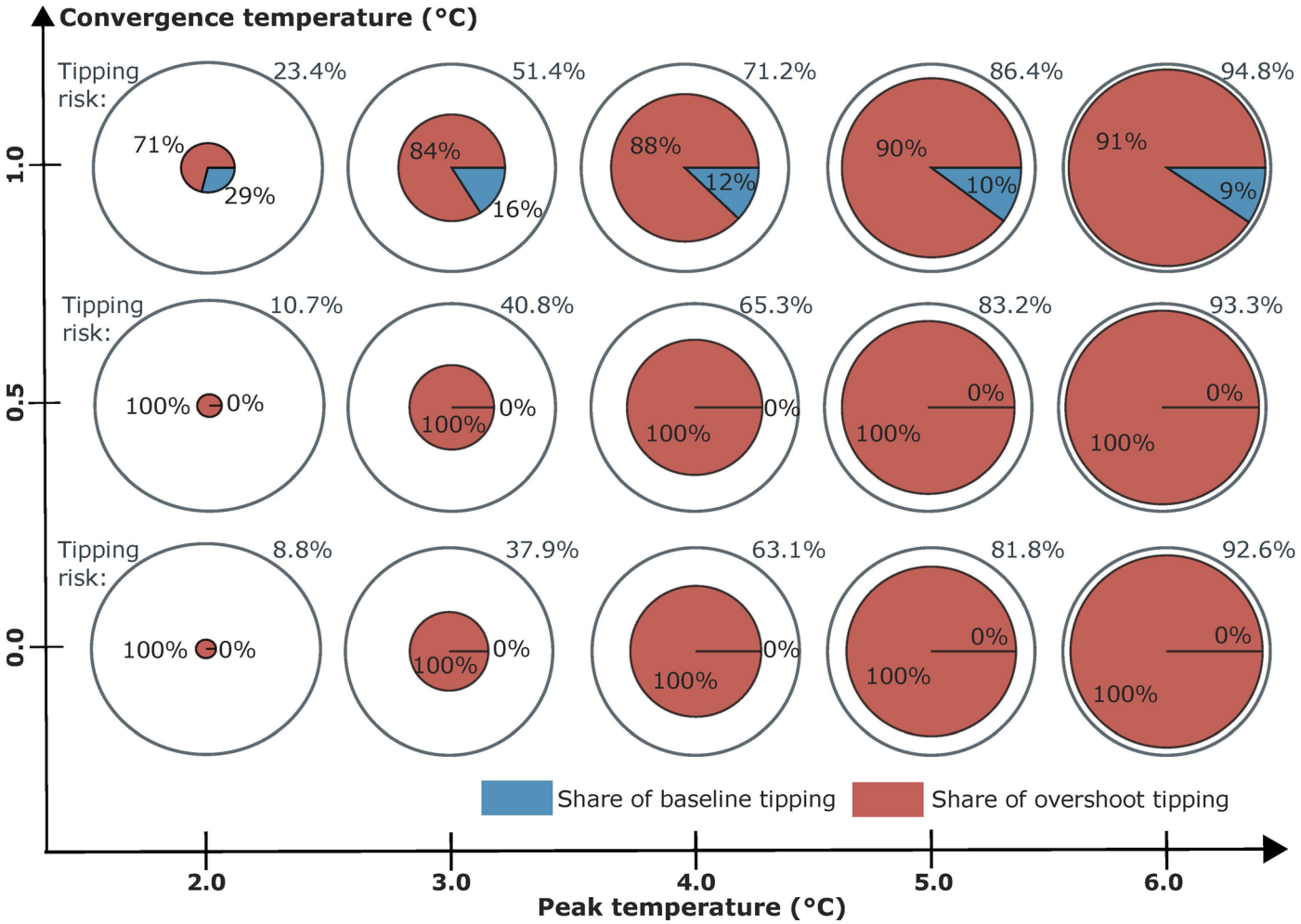

Extended Data Fig. 7 | Mechanism for tipping following a temperature overshoot for low T_Conv. Same as Fig. 4 of the main manuscript, but for lower convergence temperatures of 0.0, 0.5 and 1.0°C. To depict the tipping risk visually as the size of the pie charts, the reason (baseline or overshoot tipping) for tipping is depicted in the respective pie charts.

https://doi.org/10.1038/s41558-022-01545-9

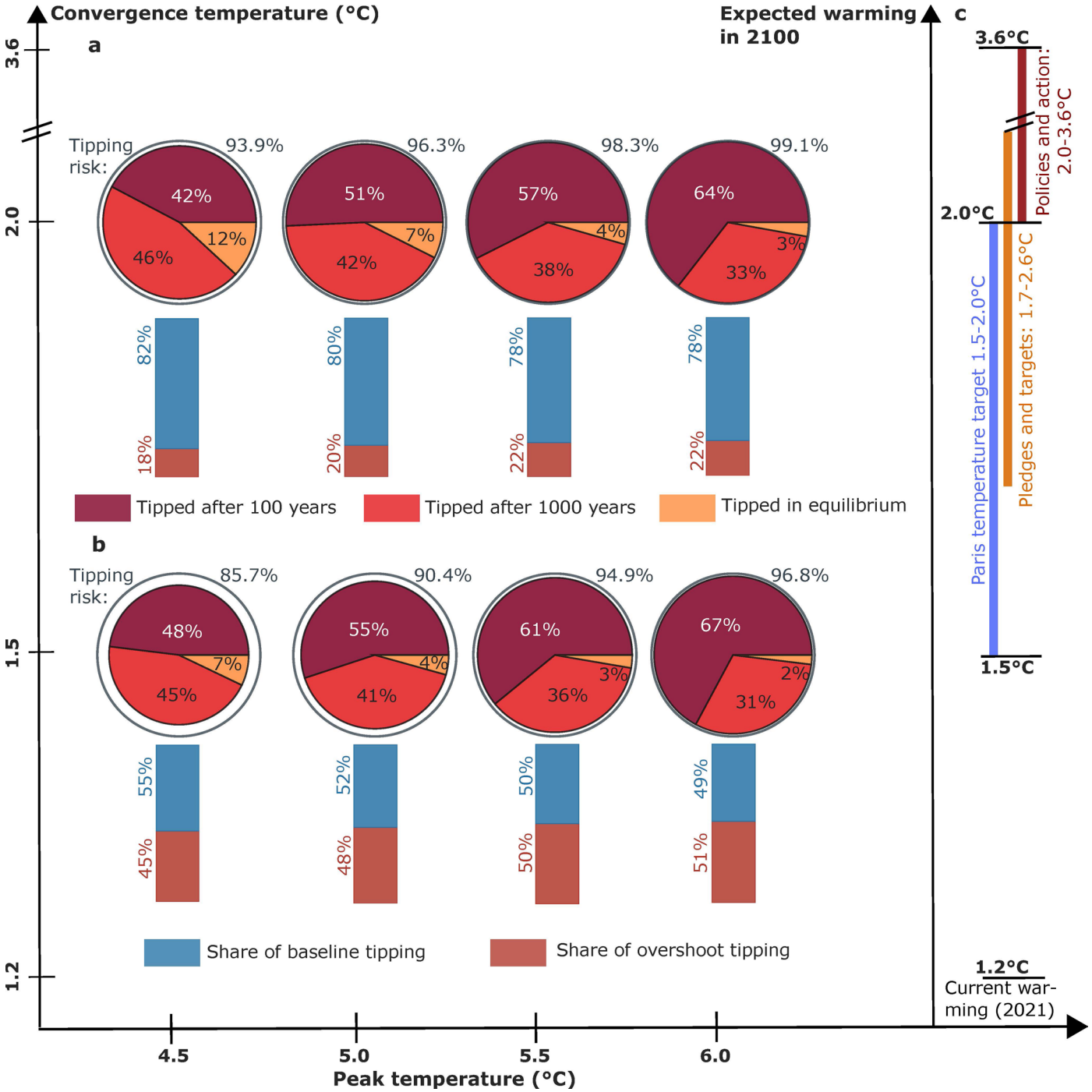

Extended Data Fig. 8 | Mechanism and timing of tipping events following a high-end temperature overshoot. Same as in Fig. 4 of the main manuscript, but for higher temperature overshoot trajectories peaking between 4.5 – 6. 0°C. In these cases, tipping also plays a very important role at shorter timescale of 100 years, see the increasing fraction of the dark red part in the pie charts. **a**, Convergence temperature of 1.5°C, **b**, Convergence temperature of 2.0°C.